

The Cryosphere Discussions is the access reviewed discussion forum of *The Cryosphere*

Layer disturbances and the radio-echo free zone in ice sheets

R. Drews¹, O. Eisen^{1,2}, I. Hamann¹, S. Kipfstuhl¹, A. Lambrecht^{1,*}, D. Steinhage¹,
F. Wilhelms¹, and H. Miller¹

¹ Alfred-Wegener-Institut für Polar- und Meeresforschung, Bremerhaven, Germany

² Institut für Umweltphysik, Heidelberg, Germany

* now at: Bundesanstalt für Geowissenschaften und Rohstoffe, Hannover, Germany

Received: 20 March 2009 – Accepted: 23 April 2009 – Published: 28 April 2009

Correspondence to: R. Drews (reinhard.drews@awi.de)

Published by Copernicus Publications on behalf of the European Geosciences Union.

TCD

3, 307–321, 2009

Radio-echo free zone in ice sheets

R. Drews et al.

Title Page

Abstract

Introduction

Conclusions

References

Tables

Figures

◀

▶

◀

▶

Back

Close

Full Screen / Esc

Printer-friendly Version

Interactive Discussion



Abstract

Radio-echo sounding of the Antarctic and Greenlandic ice sheets often reveals a layer in the lowest hundreds of meters above bedrock more or less free of radio echoes, known as the echo-free zone (EFZ). The cause of this feature is unclear, so far lacking direct evidence for its origin. We compare echoes around the EPICA drill site in Dronning Maud Land, Antarctica, with the microstructural and dielectrical properties of the EPICA-DML ice core. We find that echoes disappear in the depth range, where the coherency of the layers is lost due to disturbances caused by the ice flow. At the drill site, the EFZ onset at ~2100 m marks a boundary, below which the ice core may have experienced flow induced disturbances on various scales. The dating of the climate record becomes increasingly difficult below 1900 m, until correlation with the Dome C record is lost below 2417 m depth. The onset also indicates changing rheology which needs to be accounted for in the modeling of ice sheet dynamics.

1 Introduction

For over 40 years radio-echo sounding (RES) has been successfully applied to determine ice thickness and internal structure of large ice bodies. Internal echoes (horizons) are caused by layers contrasting significantly in the dielectric properties of the surrounding ice. The three causes for such changes are: density variations in shallow ice, acid layers and changing crystal orientation fabric (COF) in deeper ice (~>500 m) (Fujita et al., 1999). Changes in density and conductivity have isochronous character (Vaughan et al., 2004; Eisen et al., 2004). Changing COF might have isochronous character, but is also influenced by the ice flow (Eisen et al., 2007).

A commonly observed but hitherto unexplained phenomenon is the basal echo free zone (EFZ), a hundreds of meters thick band above the ice bed interface more or less free of radio echoes. An example is illustrated in Fig. 1. The absence of layering was first discussed by Robin et al. (1977) and eventually named as EFZ by Drewry and

Radio-echo free zone in ice sheets

R. Drews et al.

Title Page

Abstract

Introduction

Conclusions

References

Tables

Figures

◀

▶

◀

▶

Back

Close

Full Screen / Esc

Printer-friendly Version

Interactive Discussion



Meldrum (1978). It is often characterized by an abrupt transition and a variable upper onset. Therefore it is usually not attributed to the loss of RES sensitivity. Typically it follows the bedrock topography and increases in thickness away from ice domes (Matsuoka et al., 2003). Because direct evidence has been unavailable, it is unclear what triggers the absence of internal reflections within the EFZ, although the EFZ is observed in extensive parts of the Antarctic ice sheet (e.g. Drewry and Meldrum, 1978; Robin and Millar, 1982; Fujita et al., 1999; Siegert and Kwok, 2000; Matsuoka et al., 2003). It has been suggested by Robin and Millar (1982) that layers become increasingly deformed and tilted as the bedrock relief starts to influence stress and strain rates towards the bottom. Fujita et al. (1999) argue that variable shear over an irregular surface causes folding, mixing, and faulting of layers and thus inhibits the return of coherent reflections. Siegert and Kwok (2000) propose that recrystallization and recirculation of ice are also involved.

If the EFZ is not due to the system sensitivity, Bogorodsky et al. (1985) consider it as a proxy for the reliability of ice-core records in paleoclimate research which relies on parallel layering for the age-depth conversion. As the EFZ likely indicates a change in flow behavior, the mechanisms are also important for the modeling of ice sheet dynamics and stability (Dowdeswell and Evans, 2004).

In order to check the existing hypotheses we compare airborne RES data around the EPICA drill site in Dronning Maud Land (DML), Antarctica, with the microstructural and dielectrical properties of the 2774 m long EPICA-DML (EDML) ice core. Along with data from dielectric profiling (DEP) and the distribution of COF, we use line-scan images to visualize the integrity of layering. Line-scan images display the stratigraphy of high-scattering zones, called cloudy bands (CBs). They correlate with the impurity content of ice and we take them as a proxy for the layering of RES horizons.

So far the comparison of CB layering with RES has not been achieved, because no continuous CB stratigraphy is available for other ice cores from Antarctica. Moreover, only few CBs are seen in the deep ice cores from Byrd, Vostok, and Dome Concordia. The EDML core is the only core from Antarctica with continuous visual stratigraphy

Radio-echo free zone in ice sheets

R. Drews et al.

Title Page

Abstract

Introduction

Conclusions

References

Tables

Figures

◀

▶

◀

▶

Back

Close

Full Screen / Esc

Printer-friendly Version

Interactive Discussion



and cloudy bands which enables a direct comparison with RES data. We find that radio echoes disappear below ~2100 m at the drill site and that this transition coincides with progressive disturbances in CB-stratigraphy. We discuss possible reasons for the absence of echoes in that zone and implications for the suitability of ice for paleoclimate research and ice-sheet modeling.

2 Methods and findings

2.1 Dielectric profiling and fabric analyzer

For DEP the ice core is placed between cylindrical electrodes to measure the complex dielectric permittivity from which bulk density and conductivity can be inferred (Wilhelms et al., 1998). The electrodes were driven with a 250 kHz signal and the 1 cm electrodes were shifted along-core with a 0.5 cm increment. DEP records are corrected for variations in temperature, core diameter, and breaks. The data are scaled (Eisen et al., 2006) to the center frequency of the RES system (150 MHz). In the conductivity profile the number and height of peaks decreases towards greater depths. The last dominant peaks rising three times above the background noise occur at 2180 m. Below 2400 m the typical conductivity peaks are missing. We argue that this is partly due to diffusion but also due to geometric effects of dipped and thinned layers which aggravates the DEP record.

The fabric data are collected from thin sections between crossed polarizers (Wilson et al., 2003). The data are usually displayed in Schmidt diagrams or in terms of three Eigenvalues characterizing an ellipsoid which best approximates the c-axes distribution. Between 2025–2045 m the distribution in COF changes from a vertical girdle type to a single maximum distribution continuing to the bottom (see plots in Eisen et al., 2007). At ~2375 m the fabric resembles a vertical girdle distribution, but COF data in this depth interval is sparse.

Radio-echo free zone in ice sheets

R. Drews et al.

Title Page

Abstract

Introduction

Conclusions

References

Tables

Figures

◀

▶

◀

▶

Back

Close

Full Screen / Esc

Printer-friendly Version

Interactive Discussion



2.2 Line-scans and ice-core characteristics

The line-scan camera images 1-m segments of the ice core at a resolution of 0.1 mm (Svensson et al., 2005). While being moved along the core, the camera records light which is scattered by grain boundaries, air-bubbles and microparticles. Transparent zones appear black, and zones with inclusions appear milky.

We see progressive disturbances in CB-stratigraphy with depth (see Fig. 2) which correspond to other ice-core characteristics: above 1700 m the CBs appear straight, smooth, and parallel. They dip slightly due to the inclination of the borehole. Between ~1700–2050 m the CBs develop mm-scale undulations. From approximately 2050 m downwards the dip of CBs increases to 10–15°. Most CBs are still parallel, but mm-scaled z-folds start to develop.

Crystals with diameters larger than 10 cm are present in the last interglacial (MIS5, ~2300–2375 m) and below ~2600 m. At the transition from MIS5 to glacial MIS6 (below about 2400 m), we see a mixture of dipping and undulating CBs on various scales. In the fine-grained ice of MIS6, the CBs appear parallel, horizontal or inclined up to 30° alternated with isoclinal z-folds on the cm- to dm-scale. Below a depth of about 2400 m CBs occur with opposite sign of dip within a single core segment of 1 m length.

2.3 RES internal structure

The airborne RES system operates at a frequency of 150 MHz in a toggle mode alternately transmitting a pulse with length of 60 and 600 ns (Nixdorf et al., 1999). The theoretical vertical resolution is 5 and 50 m in ice respectively. Conversion of two-way traveltime (TWT) to depth is based on synthetic traces (Eisen et al., 2006).

Figure 1 displays two profiles in the vicinity of the drill site at Kohnen station. Profile 022150 was taken in 2002 and runs parallel to the ice divide. Profile 032137 was taken in 2003 and connects Kohnen with the German overwintering station Neumayer. Detailed internal layering is evident at both pulse lengths in the upper two thirds of the

TCD

3, 307–321, 2009

Radio-echo free zone in ice sheets

R. Drews et al.

Title Page

Abstract

Introduction

Conclusions

References

Tables

Figures

◀

▶

◀

▶

Back

Close

Full Screen / Esc

Printer-friendly Version

Interactive Discussion



ice column and prominent layers can be traced from one profile to the other. At EDML, the majority of internal reflectors below ~900 m originates from individual conductivity peaks, with some being an interference signal of closely spaced peaks (Eisen et al., 2006). The last two detected signals in the 60 ns RES data at EDML correspond to a reflector from changes in COF at 2040 m (Eisen et al., 2007) and a conductivity peak at 2080 m. The EFZ is observed in both profiles. Small signals sometimes appear within the EFZ but these are laterally usually not continuous. Figure 3a and b display an example from profile 032137, where the last continuous reflector is found at 1654 m depth, 690 m above the bed ice interface. The backscattered intensity in the long pulse data drops by 10 dB. At EDML, the EFZ is less pronounced but still evident (see Fig. 3c and d). Below about 2100 m no continuous internal layering can be found, short and long pulse data fade at similar depth, and the signal drop in the long pulse data is about 4 dB. Between 2300 and 2400 m a weak, frayed, discontinuous, and partly incoherent signal occurs in the 600 ns data. It coincides with the previously mentioned change in COF at 2375 m, and a section of undisturbed CBs below about 2385 m depth. Similar reflectors within the EFZ are also observed at other locations (Robin and Millar, 1982).

3 Physical mechanisms of the EFZ

We hypothesize that in our case the EFZ is due to the absence of suitable reflecting surfaces rather than RES sensitivity. We therefore compare data from the two different pulse lengths (600 and 60 ns, whereby in the portrayed examples the 60 ns pulse was damped by 15 dB on the system side already). The short pulse is used to detect internal layering at high vertical resolution, whereas the long pulse carries more energy and is designed for the sounding of bedrock topography. Comparing the long pulse data with the short pulse data, there is often a direct correspondence between the peaks although the short pulse layering results from interferences within a smaller vertical interval. Since both pulses are subject to the same attenuation within the ice, we argue that the long pulse has not reached its detection limit as long as layers can

Radio-echo free zone in ice sheets

R. Drews et al.

Title Page

Abstract

Introduction

Conclusions

References

Tables

Figures

◀

▶

◀

▶

Back

Close

Full Screen / Esc

Printer-friendly Version

Interactive Discussion



still be detected with the short pulse. Thus we define the EFZ's upper onset with the simultaneous disappearance of continuous layers in the 60 and 600 ns data, whereby backscattered power in the 600 ns data should drop by several dB to ensure that the long pulse has not reached its detection limit.

5 Using this technique, we identify the EFZ in many places of Fig. 1. It is evident that the EFZ's upper onset is variable in height and largely follows the bedrock topography. The onset ranges from 1600–2100 m depth, with a 600–700 m thick gap to the bedrock. Again, a loss of system sensitivity for the internal layering around 1600 m depth (e.g. Fig. 3a and b) seems unlikely, since internal layering is detected at this
10 depth in other places of the profile. One might argue that the onset represents an isotherm as it follows the bedrock topography, and hypothesize a change in temperature as the cause. However, in order to explain the sudden absence of echoes one would need a sudden increase in temperature which is not observed in the EDML borehole data (Wilhelms et al., 2006). Around the drill site (Fig. 3c and d), backscattered
15 amplitudes and signal drops are weaker. However, since long and short pulse data fade at similar depths, and the EFZ can be traced from shallower depths to the drill site, it seems likely that physical mechanisms other than the loss of system sensitivity are responsible for the absence of layering.

The DEP record changes its characteristic below about 2200 m. Conductivity peaks
20 are broader, less distinct and not as frequent. Thus a one dimensional forward model (Eisen et al., 2006) does not predict reflections within the EFZ. The lack of strong conductivity signals can be due to diffusive effects (counteracted by compression of layers) and small scale mechanical mixing lowering the dielectric contrast. However, the peak broadening can also be linked to layer dipping which is observed in
25 the line-scan data. Non-horizontal conductivity signals cause a wider and broader peak, since the DEP device integrates over the entire core diameter D along the horizontal. The magnitude of this effect can be estimated by assuming the conductivity signal $\sigma(z, x)$ to be Gaussian along the vertical z and dipped with slope m along the horizontal x . This means $\sigma(z, x) = A \exp\left(-\frac{(z-mx)^2}{d^2}\right)$, with A determining the peak

Radio-echo free zone in ice sheets

R. Drews et al.

Title Page

Abstract

Introduction

Conclusions

References

Tables

Figures

◀

▶

◀

▶

Back

Close

Full Screen / Esc

Printer-friendly Version

Interactive Discussion



amplitude and d the peak width. The integration over the core diameter D yields $\sigma(z) = \int_0^D \sigma(z, x) dx = A \frac{\sqrt{\pi d}}{2m} \left[\text{ERF} \left(\frac{m}{d} x - \frac{z}{\sqrt{d}} \right) \right]_0^D$. The magnitude of peak broadening is mainly determined by the initial peak width and the dip angle. With an exemplary peak width of $d = 1.5$ cm and a dip angle of 15° , the initial peak height decreases by $\sim 30\%$.

Thus the lack of strong conductivity peaks in the DEP record is influenced by geometric effects on the dm-scale.

We suggest that the absence of layering in the radar data is due to a larger scale layer roughness within the first Fresnel zone (diameter ~ 60 m at 2100 m depth). Not assuming a one-to-one correspondence between CB and RES reflector, we take the CB stratigraphy as a proxy for the occurrence of coherent RES reflections. Although we do find some undisturbed CBs below about 2100 m, the large majority is disturbed. The increasing waviness of the CBs suggests that the coherence of the reflected RES signals is becoming lost. In contrast, above this transition quasi-parallel layering within the first Fresnel zone results in a coherent superposition from the different parts of the propagating wave. The increasingly disturbed layering at depth reduces the coherent reflections and results in increased destructive superposition, whereby the reflection is lost. Studies about scattering on rough interfaces are often based on the Kirchhoff approximation, where random and isotropic gaussian surfaces with a specified rms-roughness and correlation length are used. In our case, we estimate that a rms-roughness of ~ 0.2 m results in ~ 10 dB loss in the specular component (Peters et al., 2005). A quantitative derivation of these parameters for the first Fresnel zone from CB disturbances seen in the ice-core is speculative. If we assume that CB-layers do not intersect (as they are isochrones) we can linearly extrapolate dipped cloudy bands in a single core segment and estimate the layer roughness and correlation length from anticipated intersection points. However, this strongly depends on which CBs are used for extrapolation and also does not boarder the parameters with an upper or lower boundary.

Although a quantitative evaluation of the layer roughness is difficult, we do think that ice flow alters the stratigraphy at EDML. Deformations on a larger scale are indicated

Radio-echo free zone in ice sheets

R. Drews et al.

Title Page

Abstract

Introduction

Conclusions

References

Tables

Figures

◀

▶

◀

▶

Back

Close

Full Screen / Esc

Printer-friendly Version

Interactive Discussion



by changing COF at the EFZ onset, and by a change in borehole geometry at 2385 m depth, when drilling was interrupted for two years during 2004 and 2006. The measured borehole closure of 2 mm/a indicates an increase in differential flow by an order of magnitude compared to the upper ice column. In the vicinity around Dome-F an EFZ is also observed. It seems to be stronger developed in the flank-flow regions than directly on the dome position (S. Fujita, personal communication, 2003, 2008), indicating an ice-dynamical link. The EDML ice core is situated in such a flank flow regime likewise as the GISP2 (Greenland Ice Sheet Project) ice core in Greenland. For GISP2, Jacobel and Hodge (1995) describe an analog coincidence of loss in internal layering in the radar data at equal depth with dipped stratigraphy in the ice core.

At EDML we think that layer roughness is the main reason for the loss of internal layering. Not enough data are at hand to generalize our results for other places in Greenland and Antarctica.

4 Conclusions

The onset of the EFZ indicates the beginning of varying flow under stronger shear, with mixing and folding of layers towards greater depth. The changing rheology needs to be accounted for in ice-sheet modeling. The EFZ marks the depth within the ice, below which paleoclimate ice-core records have to be interpreted with care. The small-scale CB features we describe may belong to disturbances on a larger scale, with overturning and thus age reversal of layers. It is likely that the disturbances are enhanced in flank flow regimes. For EDML the climate record is dated to 2417 m depth. However, Ruth et al. (2007) report increasing difficulties in matching volcanic events with the Dome Concordia record below 1900 m depth. It is hypothesized that starting at 2050 m depth, complex flow history makes the climate record less reliable until dating is impossible below 2400 m (S. Faria, personal communication, 2009).

As the EFZ is detectable from above the ice sheet, it provides an excellent indicator for internal stratigraphy for future surveys of ice-core sites, particularly for the upcoming

Radio-echo free zone in ice sheets

R. Drews et al.

Title Page

Abstract

Introduction

Conclusions

References

Tables

Figures

◀

▶

◀

▶

Back

Close

Full Screen / Esc

Printer-friendly Version

Interactive Discussion



search for the oldest ice within the framework of the International Partnerships in Ice Core Sciences (IPICS).

Acknowledgements. This work is a contribution to the European Project for Ice Coring in Antarctica (EPICA), a joint European Science Foundation/European Commission scientific programme, funded by the EU and by national contributions from Belgium, Denmark, France, Germany, Italy, the Netherlands, Norway, Sweden, Switzerland and the United Kingdom. The main logistic support was provided by IPEV and PNRA (at Dome C) and AWI (at Dronning Maud Land).

Preparation of this work was supported by the Emmy Noether-programme of the Deutsche Forschungsgemeinschaft grant EI 672/5 to O. Eisen and a scholarship of the “Evangelisches Studienwerk e.V. Villigst” to R. Drews.

References

- Bogorodsky, V., Bentley, C., and Gudmandsen, P.: Radioglaciology, D. Reidel Publishing Co., 1985. 309
- Dowdeswell, J. A. and Evans, S.: Investigations of the form and flow of ice sheets and glaciers using radio-echo sounding, Reports on Progress in Physics, 67, 1821–1861, 2004. 309
- Drewry, D. J. and Meldrum, D. T.: Antarctic Airborne Radio Echo Sounding, 1977-78, Polar Record, 19, 267–273, 1978. 308, 309
- Eisen, O., Nixdorf, U., Wilhelms, F., and Miller, H.: Age estimates of isochronous reflection horizons by combining ice core, survey, and synthetic radar data, J. Geophys. Res. – solid earth, 109, B04106, doi:10.1029/2003JB002858, 2004. 308
- Eisen, O., Wilhelms, F., Steinhage, D., and Schwander, J.: Improved method to determine radio-echo sounding reflector depths from ice-core profiles of permittivity and conductivity, J. Glaciol., 33(12), 299–310, doi:10.1029/2006GL027871, 2006. 310, 311, 312, 313
- Eisen, O., Hamann, I., Kipfstuhl, S., Steinhage, D., and Wilhelms, F.: Direct evidence for continuous radar reflector originating from changes in crystal-orientation fabric, The Cryosphere, 1, 1–10, 2007, <http://www.the-cryosphere-discuss.net/1/1/2007/>. 308, 310, 312

TCD

3, 307–321, 2009

Radio-echo free zone in ice sheets

R. Drews et al.

Title Page

Abstract

Introduction

Conclusions

References

Tables

Figures

◀

▶

◀

▶

Back

Close

Full Screen / Esc

Printer-friendly Version

Interactive Discussion



- Fujita, S., Maeno, H., Uratsuka, S., Furukawa, T., Mae, S., Fujii, Y., and Watanabe, O.: Nature of radio echo layering in the Antarctic ice sheet detected by a two frequency experiment, *J. Geophys. Res.*, 104, 13013–13024, 1999. 308, 309
- Jacobel, R. W. and Hodge, S. M.: Radar internal layers from the Greenland summit, *Geophys. Res. Lett.*, 22, 587–590, 1995. 315
- Matsuoka, K., Furukawa, T., Fujita, S., Maeno, H., Uratsuka, S., Naruse, R., and Watanabe, O.: Crystal orientation fabrics within the Antarctic ice sheet revealed by a multipolarization plane and dual-frequency radar survey, *Geophys. Res. solid earth*, 108(B10), 2499, doi:10.1029/2003JB002425, 2003. 309
- Nixdorf, U., Steinhage, D., Meyer, U., Hempel, L., Jenett, M., Wachs, P., and Miller, H.: The newly developed airborne radio-echo sounding system of the AWI as a glaciological tool, *Ann. Glaciol.*, 29, 231–238, 1999. 311
- Peters, M. E., Blankenship, D. D., and Morse, D. L.: Analysis techniques for coherent airborne radar sounding: Application to West Antarctic ice streams, *J. Geophys. Res.*, 110, B06303, doi:10.1029/2004JB003222, 2005. 314
- Robin, G. Q. and Millar, D. M.: Flow of ice sheets in the vicinity of subglacial peaks, *Ann. Glaciol.*, 3, 290–294, 1982. 309, 312
- Robin, G. Q., Drewry, D., and Meldrum, D.: International studies of ice sheet and bedrock, *Philosophical Transactions of the Royal Society of London*, 279, 185–196, 1977. 308
- Ruth, U., Barnola, J.-M., Beer, J., Bigler, M., Blunier, T., Castellano, E., Fischer, H., Fundel, F., Huybrechts, P., Kaufmann, P., Kipfstuhl, S., Lambrecht, A., Morganti, A., Oerter, H., Parrenin, F., Rybak, O., Severi, M., Udisti, R., Wilhelms, F., and Wolff, E.: “EDML1”: a chronology for the EPICA deep ice core from Dronning Maud Land, Antarctica, over the last 150 000 years, *Clim. Past*, 3, 475–484, 2007, <http://www.clim-past.net/3/475/2007/>. 315
- Siegert, M. and Kwok, R.: Ice-sheet radar layering and the development of preferred crystal orientation fabrics between Lake Vostok and Ridge B, central East Antarctica, *Earth Planet. Sci. Lett.*, 179, 227–235, 2000. 309
- Svensson, A., Nielsen, S. W., Kipfstuhl, S., Johnsen, S. J., Steffensen, J. P., Bigler, M., Ruth, U., and R  thlisberger, R.: Visual stratigraphy of the North Greenland Ice Core Project (NorthGRIP) ice core during the last glacial period, *J. Geophys. Res.*, 110, D02108, doi:10.1029/2004JD005134, 2005. 311
- Vaughan, D. G., Anderson, P. S., King, J. C., Mann, G. W., Mobbs, S. D., and Ladkin, R. S.:

TCD

3, 307–321, 2009

Radio-echo free zone in ice sheets

R. Drews et al.

Title Page

Abstract

Introduction

Conclusions

References

Tables

Figures

◀

▶

◀

▶

Back

Close

Full Screen / Esc

Printer-friendly Version

Interactive Discussion



Imaging of firn isochrones across an Antarctic ice rise and implications for patterns of snow accumulation rate, J. Glaciol., 50, 413–418(6), doi:10.3189/172756504781829882, 2004. 308

- 5 Wilhelms, F., Kipfstuhl, S., Miller, H., Heinloth, K., and Firestone., J.: Precise dielectric profiling of ice cores: A new device with improved guarding and its theory, J. Glaciol., 44, 171–174, 1998. 310
- 10 Wilhelms, F., Sheldon, S. G., Hamann, I., and Kipfstuhl, S.: Implications for and Findings from Deep Ice Core Drillings An Example: The Ultimate Tensile Strength of Ice at High Strain Rates, vol. 311, The Royal Society of Chemistry Special Publication, 2006. 313
- Wilson, C. J. L., Russell-Head, D., and Sim, H. M.: The application of an automated fabric analyzer system to the textural evolution of folded ice layers in shear zones, Ann. Glaciol., 37, 7–17(11), doi:10.3189/172756403781815401, 2003. 310

TCD

3, 307–321, 2009

Radio-echo free zone in ice sheets

R. Drews et al.

Title Page

Abstract

Introduction

Conclusions

References

Tables

Figures

◀

▶

◀

▶

Back

Close

Full Screen / Esc

Printer-friendly Version

Interactive Discussion



Radio-echo free zone in ice sheets

R. Drews et al.

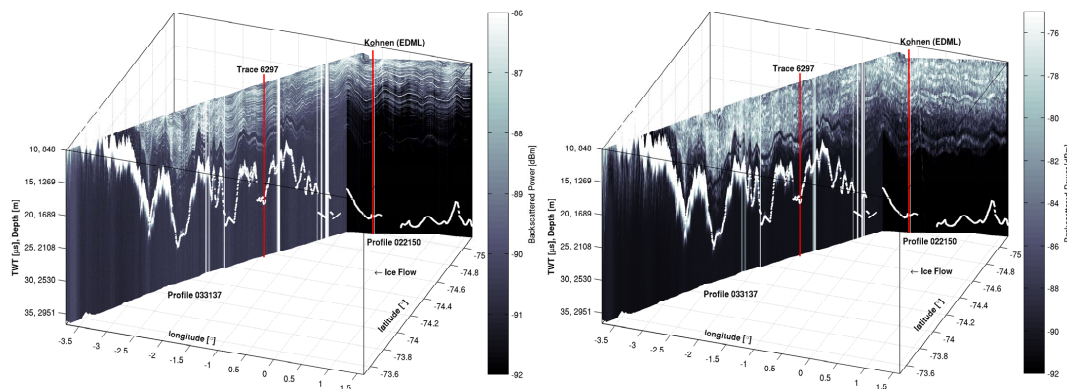
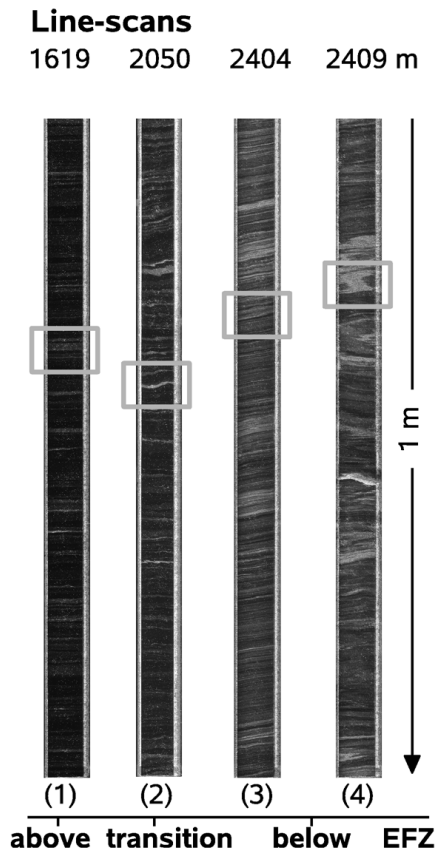


Fig. 1. Radar profiles in the vicinity of Kohnen station recorded with the 60 ns (left) and 600 ns (right) pulse. Bedrock was picked from differentiated data. The TWT is corrected to the first break of the surface reflection. For better visibility of deeper layers the upper layers have been excluded. Profile 022150 has a length of 40 km and runs parallel to the ice divide. Ice flow is approximately 1 m/a. Profile 033137 has a length of 200 km and intersects the Kirwanveggen mountain range. Although the upper boundary of the EFZ cannot be mapped everywhere, it is clearly visible that it is variable in height and follows the bedrock topography. Traces shown in Fig. 3 are labeled at the top.

[Title Page](#)[Abstract](#)[Introduction](#)[Conclusions](#)[References](#)[Tables](#)[Figures](#)[I◀](#)[▶I](#)[◀](#)[▶](#)[Back](#)[Close](#)[Full Screen / Esc](#)[Printer-friendly Version](#)[Interactive Discussion](#)



Zoom

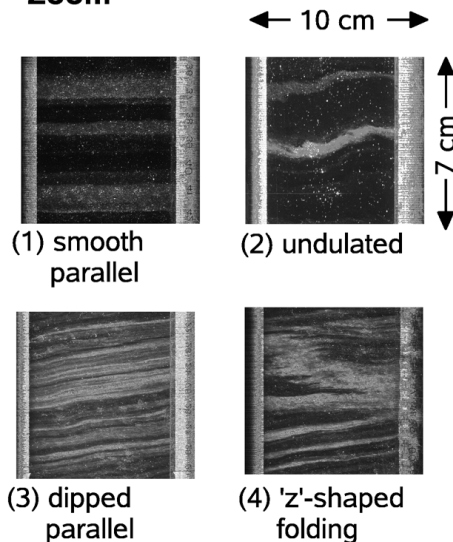


Fig. 2. Line-scan images of the EDML ice core (left) with zoom on the right. Cloudy band stratigraphy appears undisturbed above EFZ (1) whereas in the transition zone mm-scale undulations start to develop (2). Within the EFZ, layers appear partly dipped parallel (3) and partly rough (4) as dips point into opposite directions. Dips can be intersected with z-shaped folds (zoom of 4).

Radio-echo free zone in ice sheets

R. Drews et al.

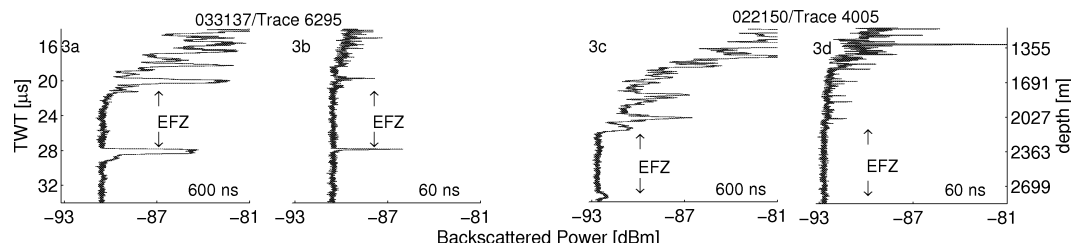


Fig. 3. The EFZ is identified by the simultaneous disappearance of continuous layers in the 60 and 600 ns data, whereby backscattered power in the 600 ns data drops by several dB, **(a)** and **(b)** trace 6295 (profile 033137) of 600 and 60 ns data is a typical example for the EFZ. The last continuous signal is visible at $20.1\ \mu\text{s}$ in the 600 ns and at $19.7\ \mu\text{s}$ ($\sim 1654\ \text{m}$ depth) in the 60 ns pulse. Bedrock is clearly visible in both traces at $27.9\ \mu\text{s}$ ($\sim 2344\ \text{m}$ depth). **(c)** and **(d)** trace 4205 (profile 022150) for both pulses at the EPICA drill site. Bedrock is visible in both traces at about $2790\ \text{m}$ depth. Last continuous signals above the bedrock are detected at 25.4 and $25\ \mu\text{s}$ TWT ($\sim 2100\ \text{m}$ depth). Because of the larger depth, the signal drop in the 600 ns data is smaller than in Fig. 2a, but still significant.

Title Page

Abstract

Introduction

Conclusions

References

Tables

Figures

◀

▶

◀

▶

Back

Close

Full Screen / Esc

Printer-friendly Version

Interactive Discussion

